Energy Density of Cylindrical Li-Ion Cells: A Comparison of Commercial 18650 to the 21700 Cells

Jason B. Quinn,* Thomas Waldmann,z Karsten Richter,** Michael Kasper, and Margret Wohlfahrt-Mehrens**

ZSW - Zentrum für Sonnenenergie- und Wasserstoff-Forschung Baden-Württemberg, D-89081 Ulm, Germany

The standard format for cylindrical Li-ion cells is about to change from 18650-type cells (18mm diameter, 65mm height) to 21700-type cells (21mm diameter, 70mm height). We investigated the properties of five 18650 cells, three of the first commercially available 21700, and three types of the similar 20700 cells in detail. In particular, the (i) specific energy/energy density and electrode thickness, (ii) electrode area and cell resistance, (iii) specific energy as a function of discharge C-rate, as well as (iv) heating behavior due to current flow are analyzed. Finally, the production effort for cells and packs are roughly estimated for 21700 cells compared to 18650 cells.

 [DOI: 10.1149/2.0281814jes]

Manuscript submitted August 20, 2018; revised manuscript received October 5, 2018. Published October 19, 2018.

The lithium ion battery was first released commercially by Sony in 1991,[1,2] featuring significantly longer life-time and energy density compared to nickel-cadmium rechargeable batteries. In 1994, Panasonic debuted the first 18650 sized cell,[3] which quickly became the most popular cylindrical format. Besides cylindrical cells (e.g. 18650, 26650), Lithium ion technology is implemented in a variety of formats depending on their application: coin (e.g. CR2032, CR2016), pouch, and prismatic. The majority of electric vehicle (EV) manufacturers elect to use larger prismatic cells,[4] whereas Tesla had adopted 18650-type cells, which were produced in billions per year worldwide.

Today, Panasonic supplies Tesla with cells for the Model S, 3, and X. The companies initially worked to establish the 20700 cell format as a new standard for use in electric vehicles, however, it was abandoned in favor of the 21700 format. An increase in cell size allows for a larger jellyroll, in both width and increased number of windings, therefore increasing electrode area (see Figure 1 for size comparison). The larger 21700 format was adopted by other manufacturers and has since become a new modern standard.[5]

Currently, a few different types of 20700 and 21700 cells are available commercially, however, to best of our knowledge there are no published scientific investigations on these cells. Furthermore, in different discussions, we found that there is a controversy on an increase of energy density by the cell format and a need to clarify this topic on a scientific basis. Therefore, in this work we wish to shed some light on the new format and its potential impact. To do this, we compared several commercial 18650, 20700, and 21700 cells (see Table I).

In this paper, energy content, specific energy, cell performance, internal resistance, and heating behavior during current flow will be measured and correlated to electrode thickness and area. Based on the results and in first approximation, we will also briefly discuss possible production benefits of 21700 format over 18650.

Experimental

The various cell types evaluated in this study are shown with respective energy, energy density, specific energy, dimensional data, and voltage range in Table I. In order to identify cells we use a naming scheme structured as [cell size]-[letter assigned to manufacturer][cell type]. For example, 20700-E1 and 21700-E1 are different cells from the same manufacturer. Energy density values are based on nominal dimensions according to each cell's data sheet. Please note that the cell dimensions are not exactly the same as expected for the different cell formats. For instance, the mean diameter of 18650 and 21700 cells is 18.08 mm and 21.19 mm instead of 18.0 mm and 21.0 mm, respectively.

*Electrochemical Society Member.
**Electrochemical Society Student Member.
zE-mail: thomas.waldmann@zsw-bw.de

All cells were first of all tested as delivered regarding their mass, voltage, and internal resistance (Hioki 3554, 1 kHz). Table II shows the mean values and the standard deviations. The low standard deviations indicate that all cells are suitable for further tests.

In order to yield the coating thicknesses shown in Figure 2, the cells were discharged to their respective end-of-discharge voltages before disassembly in a fume hood. The electrodes were separated and washed three times for 1 minute in DMC. After drying, the thicknesses of the coatings were measured by a micrometer gauge. The mean value of ten positions per cell were used in Figure 2. The X-ray computed tomography image shown in Figure 3 was obtained for cell type 21700-G1 with a v|tome|x 300. We note that cell types 18650-A2 (1.2Ah) and 18650-A3 (2.2 Ah) were only used in Figure 2 and Figure 5.

For Figure 5a, two cells of each type were discharged and charged three times at 0.5C (CC-CV until I<C/10), and their resistances were measured twice after a break (>30min) in the charged state at room temperature. Pouch cells with different electrode numbers (Figures 5b and 5c), were built from NMC cathodes, graphite anodes, a Celgard Separator (2325), and EC:EMC = 3:7 (wt-%), 2% VC, 1M $LiPF_6$ as electrolyte.

All electrochemical tests were performed by a BaSyTec XCTS equipped with 25A channels at 25°C in climate chambers (Vötsch). Rate capability tests were performed by CC-CV charging at 0.5C to 4.2V, ending when I < C/10, and CC discharge ending at the respective cutoff voltage. A 30 minute pause was placed between each step to allow for voltage relaxation. Discharge rates of 0.5C, 1.0C, 1.5C, 2.0C, 2.5C, 3.0C, 3.5C, and 3.75C were used for all cells. Repetition of all tests with a second cell showed very good reproducibility. Those which exhibited great rate capability and lower heating (high power

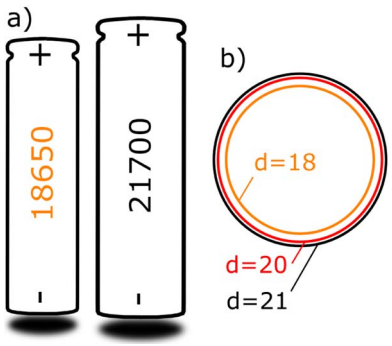

Figure 1. Size comparison of 18650 cells (h = 65mm, d = 18mm), 20700 cells (h = 70mm, d = 20mm), and 21700 cells (h = 70mm, d = 21mm). a) side view, 20700 cells are not shown since their side view is very similar to 21700 cells. b) Comparison of cell diameter, (b) not in scale with (a).

Table I. Overview on investigated cells.

Cell type	Energy per cell/Wh	Energy density/Wh/l	Specific energy/Wh/kg	h/mm	d/mm	Cutoff Voltage/V	Charge Voltage/V
18650-A1	5.13	314.4	114.0	64.99	17.88	2.0	4.2
18650-B1	9.13	538.7	206.2	65.02	18.22	2.0	4.2
18650-C1	11.23	670.0	231.5	65.14	18.14	2.5	4.2
20700-D1	14.54	663.5	237.5	70.04	19.96	2.5	4.2
20700-E1	10.55	466.8	169.9	69.96	20.28	2.5	4.2
20700-F1	14.65	668.4	232.6	70.06	19.96	2.5	4.2
21700-E1	13.15	519.1	207.1	70.27	21.43	2.5	4.2
21700-G1	16.77	684.2	239.5	69.71	21.16	2.0	4.2
21700-H1	16.32	672.1	236.5	70.25	20.98	2.5	4.2

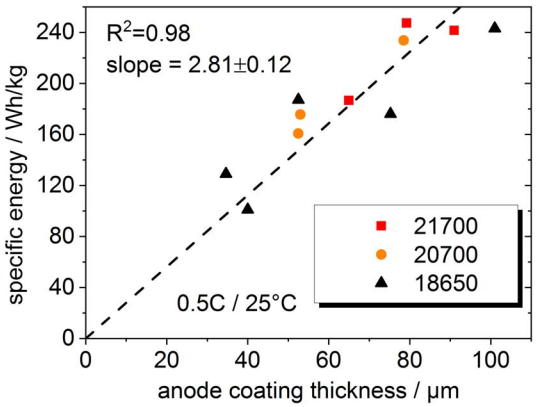

Figure 2. Correlation of specific energy of commercial cylindrical cells as a function of anode coating thickness measured after Post-Mortem analysis. The fit was forced through the origin. Values were obtained at 0.5C discharge rate and 25°C.

Table II. Measured specifications of investigated cells. Data are mean values and standard deviations. In case of cell 21700-G1 only 2 cells were available, therefore the errors from the measurement devices were taken instead of the standard deviation.

Cell Count	Cell Type	Capacity/ Ah	m/g	U/V	R_i/mΩ
100	18650-A1	1.50	42.23 ± 0.10	3.77 ± 0.01	16.2 ± 0.3
30	18650-B1	2.50	48.79 ± 0.07	3.47 ± 0.01	10.4 ± 0.2
20	18650-C1	3.40	46.29 ± 0.06	3.53 ± 0.01	10.4 ± 0.2
20	20700-D1	4.25	62.16 ± 0.06	3.50 ± 0.01	14.8 ± 0.2
20	20700-E1	3.03	58.06 ± 0.31	3.64 ± 0.02	11.5 ± 0.4
40	20700-F1	4.25	62.06 ± 0.07	3.65 ± 0.01	14.8 ± 0.1
20	21700-E1	3.75	70.45 ± 0.62	3.87 ± 0.02	13.6 ± 0.3
2	21700-G1	5.00	68.46 ± 0.06	3.45 ± 0.01	14.0 ± 0.2
20	21700-H1	4.80	67.57 ± 0.09	3.58 ± 0.01	15.0 ± 0.2

cells) were subject to discharge rates up to 12C, and the maximum channel current of 25A. Cell surface temperature was measured by taping an NTC-type temperature sensor (error: ±1°C) on the middle of the cell can, where a ∼1.5 × 2.0 cm^2 piece of plastic mantle was removed.

Results and Discussion

Energy density and electrode thickness.—Figure 2 shows a clear correlation between anode coating thickness from Post-Mortem analysis with specific energy on cell level. The anode was chosen for this analysis since the material (graphite) is expected to be more similar in the different cells from different manufacturers, while the cathode materials may vary (different types of NMC, NCA, . . .). In particular, for cell types 18650-A1, 18650-A2, 18650-A3, and

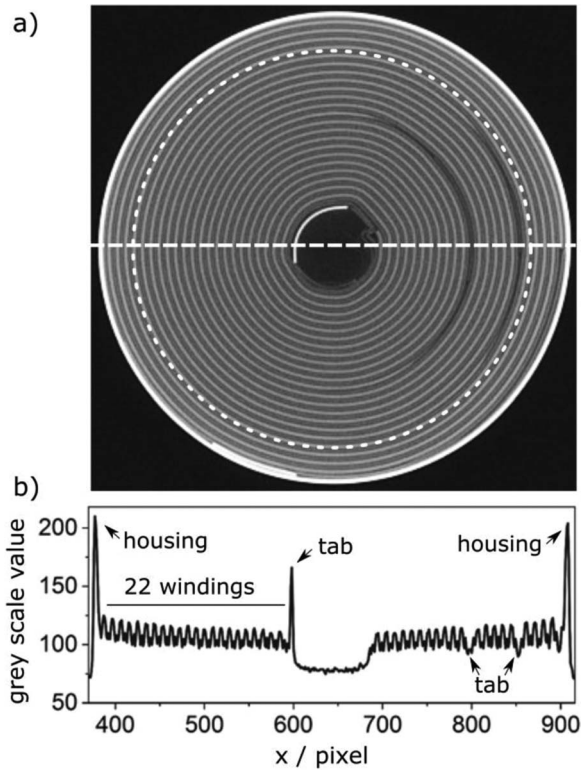

Figure 3. a) 2D CT cross-section at mid-height of cell type 21700-G1, b) 1D CT cross-section along the broken line in (a). The dotted circle shows the diameter of a 18650-type cell for comparison. White/grey/black in (a) correspond to high/mid/low gray scale values in (b).

18650C1, the cathode chemistry is NMC111/LMO,[6,7] LMO,[7] NMC532,[7] and NCA,[7,8] respectively, which obviously does not change the trend for the anode in Figure 2.

The data points in Figure 2 for both, the 18650 and 21700 cells show a similar correlation and scatter around a linear fit with $R^2 = 0.98$. We note that this fit is forced through the origin which is physically meaningful, since a hypothetical cell with no anode coating has a specific energy of 0. In contrast to the cells with high specific energy (right upper corner of Figure 2), the cells with lower specific energy are typically high-power cells (left lower corner). Please note that the trend for energy density is similar.

The scattering in Figure 2 originates from various factors, which are summarized in Table III. Differences in cell design[9–11] (tab design, cap), separator[12] (thickness, material, porosity, tortuosity), electrodes[13,14] (loading, porosity, tortuosity, collector foil material/thickness, N/P ratio), materials[14,15] (active materials type, stoichiometry, electrolyte/additives, conductive salt, SEI, binder, particle size distribution) which are likely to be present in the different commercial cell types. For example, more than one tab is

Table III. Possible influences on specific energy of a Li-ion cell.

Group	Influence parameter
cell design	tab design
	current collectors
	cap
separator	thickness
	material
	porosity
	tortuosity
electrodes	loading
	porosity
	tortuosity
	collector foil material/thickness
	N/P ratio
materials	active materials type
	stoichiometry
	electrolyte/additives
	conductive salt
	SEI
	binder
	particle size distribution

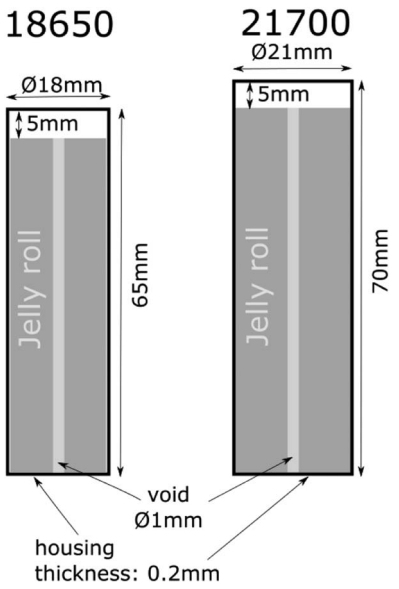

Figure 4. Cylinder volumes used for the estimation of energy densities for 18650 and 21700 cells.

favorable for the electrical homogeneity,[10] internal resistance,[9] discharge capacity,[11] and heating behavior[9,11] of high-power cells. Additionally, uncertainties in the measurement of the anode thicknesses must be taken into account.

Please note that the anode coating thicknesses in Figure 2 were obtained from Post-Mortem analysis of commercial cells discharged to their respective end-of-discharge voltage (see Table I). In this process, the cell housing is removed and therefore potential pressure on the jellyroll is released. Consequently, the measured thicknesses are not exactly the same as in the closed cells since they might have slightly expanded. Furthermore, during washing of the electrodes with DMC, material might have been removed which would lead to a lower thickness. However, a comparison with a 2D CT cross-section of cell type 21700-G1 (Figure 3a) showed a reasonable agreement. From 50 measurements of the periodical distance from the CT image, a mean value of 371 ± 13 µm was obtained. Additionally, Figure 3b shows a 1D CT cross-section where 22 windings (22 maxima) can be counted. The mean periodical distance between each winding was calculated to be 376 ± 23 µm and an inner cell diameter of 20.7 mm was determined using the local minima adjacent to each housing peak. This is in the same range as the sum of the thickness of anode, cathode, and 2x separator obtained for the same cell type from Post-Mortem analysis (366 µm).

It is noted that the 2D CT cross-section in Figure 3a looks similar to that of 18650 cells.[7,16–20] The dotted circle in Figure 3a shows the diameter of a 18650 cell for comparison. It can directly be seen that for the same thickness of anode, cathode, and separator, less windings could be achieved. In this case (366 µm periodic distance) the 21700 cell can accommodate ∼4 more windings. This is based on the assumption that the space utilization at inner and outermost electrode ranges is always optimized in the same manner. For thinner electrodes the number of additional windings will be higher. Additionally, please note that the extra outer windings of the 21700 cells contribute more to the energy content of the cells compared to the inner windings which would be also present an a similar 18650 cell. According to the Archimedean spiral[21] the increase of lengths of the electrodes is disproportionately higher for outer windings.

It also has to be considered that the measured anode coating thicknesses in this paper are not the same as for the coated and calendared electrodes in the production process before being built into the cells, since soaking with electrolyte and cell formation are likely to lead to a thickness increase.

Nevertheless, the high R^2-value for the linear fit in Figure 2 shows that in spite of the differences in the cells discussed above, the main trend for higher specific energy is higher electrode thickness. This trend holds for all three cell formats – 18560, 20700, and 21700 – and from different manufacturers. I.e. the specific energy of cells with comparable electrode thickness is similar for all three cell formats. This implies, that for similar anode coating thicknesses, the main changing parameter when going from 18650 to 21700 will be the energy content of the cells and not specific energy or energy density. Indeed, a straightforward calculation based on reasonable cylinder volumes for 18650 and 21700 shows that the energy content is increased by ∼49%, whereas the energy density increases by only ∼2%. In this very basic calculation the volume of the jelly roll (excluding the empty volume in the core) is used as a measure for the energy content and compared with the total outer volume of the cells (energy density) which are treated as mathematically perfect cylinders (for measures see Figure 4). We note that this is a rough estimation which is only valid if usage of volume inside cells is not enhanced by changing the cell format.

The estimation of energy content was cross-checked by measuring the lengths of the windings in the CT image (Figure 3a). Comparison of the length of all windings (21700 cell) with the inner windings (18650 cell) and correction by a factor taking the heights of the cell types into accounts yielded again 49% of energy increase and is therefore in total agreement with the estimation by cylinder volumes. Considering the fact that the outer windings contribute strongly to the cell capacity it is not surprising that the outer diameters given in Table I are in some cases higher than expected from the numbers in the cell format.

The anode thickness in cylindrical cells with common materials can be estimated by the slope of Figure 2 as

$$\mathrm{d}\ [\mu m] = \frac{\text{specific energy [Wh/kg]}}{2.81 \pm 0.12} \qquad [1]$$

Recently, Muenzel et al. tested five different types of 18650 cells which had charge capacities in the range of 3.07Ah to 4.9Ah.[22] Three of these 18650 cells rated below 3.35Ah were produced by major manufacturers and performed above 93% of their rated capacity.[22] In contrast, two cheaper cell types which were rated with unusually high values of 4.2Ah and 4.9Ah performed very poorly with only 18% and 12% of their rated capacity, respectively.[22] From our results it is likely that these cheaper cells investigated by Muenzel et al.[22] were built to have theoretically increased capacities by thicker electrode coatings. By using Eq. 1 we roughly estimate a coating thicknesses for the anode of ∼166 ± 10 µm (based on 469.0 Wh/kg = 4.2Ah × 3.6V/32.24g and 464.4 Wh/kg = 4.9Ah × 3.6V/37.98g,[22] with the assumption of 3.6V as nominal voltage). Our estimation of the high coating thicknesses in the 4.2Ah and 4.9Ah cells reported by

Muenzel et al. are in accordance with high ohmic cell resistances[22] and short electrode lengths[23] of these cells. It is likely that the coating thicknesses of the electrodes in these cells exceed a critical limit leading to effectively lower specific energies, i.e. a decrease of the practically usable capacity.[24]

Therefore, it is very likely that the correlation in Figure 2 should become non-linear (more flat) with a transition above ~90µm (~240Wh/kg), which is in accordance with simulations by Du et al. who calculated such a curve shape[25] and with results by others who investigated thick electrodes.[22,24,26] It was also reported that the curve shape depends on the discharge C-rate.[24,25] I.e. Singh et al. reported that the capacity increases with electrode thickness up to 305 µm for C/10, however there are maxima e.g. for C/5 and C/2 at 255µm and 205µm, respectively.[24] Therefore, Eq. 1 describes only the relation for anode coating thicknesses up to ~90µm and the corresponding practical specific energies for 18650, 20700, and 21700-type cells with common materials at 0.5C/25°C.

The reason for this deviation at anode coating thicknesses above ~90µm is most likely that the inner part of the active material in the coating (near the current collector) is underutilized at very high electrode loadings.[25,26] Danner et al. presented experiments and simulations on the performance of Li-ion cells with electrodes of different thickness with discharge rates in the range of C/10 to C/2.[26] In that study, cells with coating thicknesses of 70µm showed a significantly better performance than cells with 320 µm coating thickness.[26] This fits to the trend discussed above. Danner et al. attributed this performance loss for thicker NMC electrodes to a strong limitation of the transport of Li ions in the electrolyte, which was expressed in a vanishing of the Li ion concentration in the cathode near to the current collector.[26] Du et al. came to the same conclusion for NCA cathodes.[25]

The higher specific energy as a function of thicker anode coating in Figure 2 originates from a better ratio of active/inactive materials and is likely to be the most important factor for conventional electrodes. Obviously, this trend in Figure 2 is the same for 18650, 20700, and 21700 cells. Therefore, the 20700 and 21700 cells do not show a significant increase of specific energy compared to 18650 cells which would originate from the size difference. A stronger difference is observed between cells of the same format which are optimized either for high energy or for high power.

Influences on cell resistance.—Figure 5a shows the cell resistance for different commercial cylindrical cells as a function of capacity. It can be seen that the data points of the 18650 cells mostly form one group and those of the 20700 and 21700 cells form a second group. We note that one of the points (18650-B1) is an outlier cell. We are currently investigating the reason the lower resistance of this cell type.

The resistances of the 18650 cells are systematically higher compared to the 20700 and 21700 cells. Within both groups, the cell resistance rises as a function of discharge energy. The reason is that higher discharge energies are achieved by thicker electrode coatings (see Figure 2 and Eq. 1), which lead to shorter electrodes and consequently to smaller total electrochemically usable electrode areas at a given cell diameter. An additional contribution is related to the resistance rise due to higher electrode thickness,[27] however, this cannot be directly seen from Figure 5a. Unfortunately, the resistance values given in literature cannot be directly compared with our results, since they were not measured with the same method.

Again, we observed clear trends including some scattering of the data. The reason for the deviations from the trend are based on electrolyte, electrode porosity, active materials, binder, and particle size distributions as summarized in Table III.

The trend of the lower resistances for the larger 20700 and 21700 cells can be explained by the larger electrode areas due to larger cell diameters. Figure 5b shows the cell resistances of stacked lab pouch cells (<1.5Ah) as a function of the number n of cathodes in the stack. It can clearly be seen that the cell resistance decreases with n and therefore with the total cathode area in the cell. The decrease fits very well to a hyperbola (see inset of Figure 5b) in analogy to

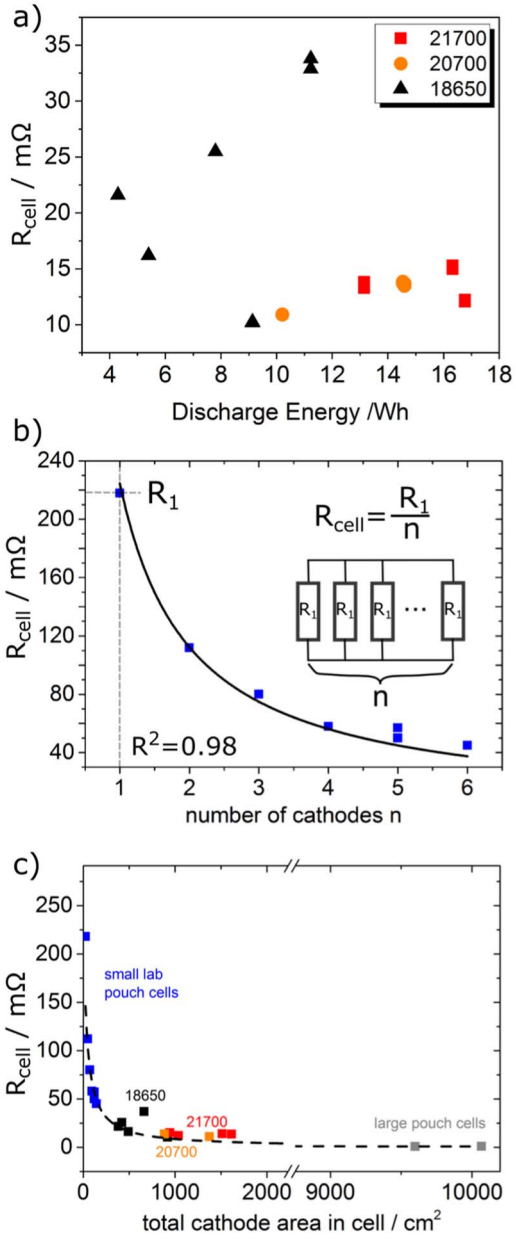

Figure 5. a) Cell resistance of cylindrical cells with different formats as a function of cell capacity. b) Cell resistance as a function of the number of electrodes in stacked lab pouch cells. The inset shows the analogy to resistors connected in parallel. c) Cell resistance as a function of total cathode area in different types of lab and commercial cells.

resistors connected in parallel. This resistive behavior of a cell with electrode areas connected in parallel is very similar to cells connected in parallel.[28]

Figure 5c shows the resistances of the stacked lab pouch cells together with very different types of commercial cells as a function of coated cathode area. The cathode area was chosen in this evaluation since it is limiting the cell capacity. It can clearly be seen that the resistances of all these very different types of cells (small lab pouch cells, 18650, 20700, 21700, large pouch cells) follow a similar rule as in Figure 5b. One difference between these cell formats are the positive temperature coefficient (PTC) resistors which are usually only implemented in cylindrical cells. However, the effect of the coated cathode areas seems to be much stronger than the resistance of the PTCs.

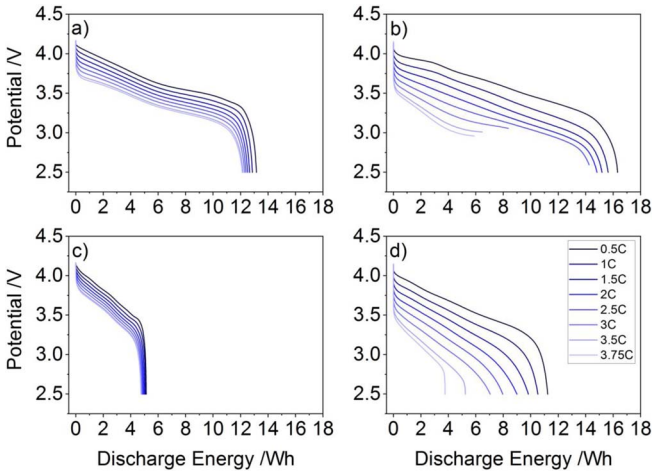

Figure 6. Discharge voltage curves for 21700 a) high power: 21700-E1, b) high energy: 21700-H1, and 18650 c) high power: 18650-A1, and d) high energy: 18650-C1 cells, with anode thicknesses of 65μm, 91μm, 34μm, and 101μm, respectively.

Rate capability tests.—Figures 6a–6d shows exemplarily the discharge curves at high C-rates for 21700 high power, high energy, and 18650 high power, and high energy cells, with anode thicknesses of 65 μm, 91 μm, 34 μm, and 101 μm, respectively. The longer path for e^- to travel through the conductivity network (graphite, conductive carbon) as well as the diffusion path for Li^+ through of the pores of a thicker electrode in Figure 6b) and Figure 6d) result in faster energy loss and lower average voltage at high C-rates than in Figure 6a) or Figure 6c). Our experimental results with commercial cells are in accordance with simulations of 18650 cells by Du et al. who investigated cathode thicknesses ranging from 60 μm to 240μm.[25] Different thicknesses showed little to no capacity loss up to C/2, but saw marked differences at higher rates.[25] 240μm showed nearly 50% lower discharge energy than 60μm at 1C, and just over 12.5% of the capacity at 2C in simulations.[25] This is exemplified in our experimental results at 3.75C where the cell in Figure 6d) reaches ∼33% of its original discharge energy, and the cell in Figure 6c) still retains ∼93%. Singh et al. also studied the effects of electrode thickness of single layer NMC pouch cells, increasing anode and cathode thickness from 70μm to 305μm.[29] At C/5 virtually no capacity loss was observed, however, noticeable increase was seen in overpotential with increasing electrode thickness in both charging and discharging curves.[29]

Ohmic losses due to electron conductivity and lithium transport through the pores become more prominent in thicker electrodes.[29] Indeed we also observe an increased overpotential for cells with thicker electrodes. At higher discharge rates, the initial voltage drops of the cells in Figure 6b) and Figure 6d) become more significant than for the high power cells.

To better visualize rate capability, Figure 7a plots the total discharge energy of all cells as a function of discharge C-rate. Cells having higher initial discharge capacity within the same format show a steeper decline in available capacity with increasing discharge rate. Cell 18650-C1 has the highest anode coating thickness at 101μm, and shows by far the worst rate capability, with available energy dropping off sharply around 2.5C. We suspect that his behavior is related to very low porosity of the anodes from this cell.

From Figure 7a, the clear trend of an upper limit for the rate capability can be seen. This trend can be fit by line (broken line, slope = –0.35, $R^2 = 0.96$). Here is has to be discussed that cells with higher energy content can deliver higher absolute currents. Therefore, Figure 7b shows the same data plotted against absolute currents. It can be seen that the higher energy contents compensate the rate capability only partly.

Figures 7a and 7b are superimposed with data with the temperatures at the end of discharging. Near the broken lines in Figures 7a and 7b, a rise of the cell surface temperature can be observed. Therefore, the temperature rise of the cells due to current flow are a limiting factor for rate capability. This limit is valid for all tested cells in this study, independent from the cell format.

Heating of cells due to current flow.—Figure 8 shows exemplarily the rate-dependent surface heating of 21700 a) high power, b) high energy, and 18650 c) high power, and d) high energy cells, with anode thicknesses of 65 μm, 91 μm, 34 μm, an 101 μm. High energy cells with thicker anodes show substantially increased heating during discharge. Ohmic resistances as well as polarization and reaction heat in the cells[30] cause a loss of power as waste heat, and in turn, lower discharge energy. We note that discharge tests were automatically stopped if the cell surface temperature reached 65°C, which is higher than the manufacturer's stated maximum (typically 60°C). For example, the cell in Figure 8b) was unable to safely complete discharging past 2C due to excessive heat generation.

Zhao et al. performed simulations of LMO/graphite cells to study thermal and electrochemical effects of varying electrode thickness.[27] In accordance with our results, the authors found that cells with thicker electrodes experienced more intensive and uneven temperature responses mostly due to ohmic heat generation.[27] Thicker electrodes showed lower power output due to longer diffusion distances and concentration polarization, and diffusion limitation in thicker cells resulted in underutilized active materials.[25,26]

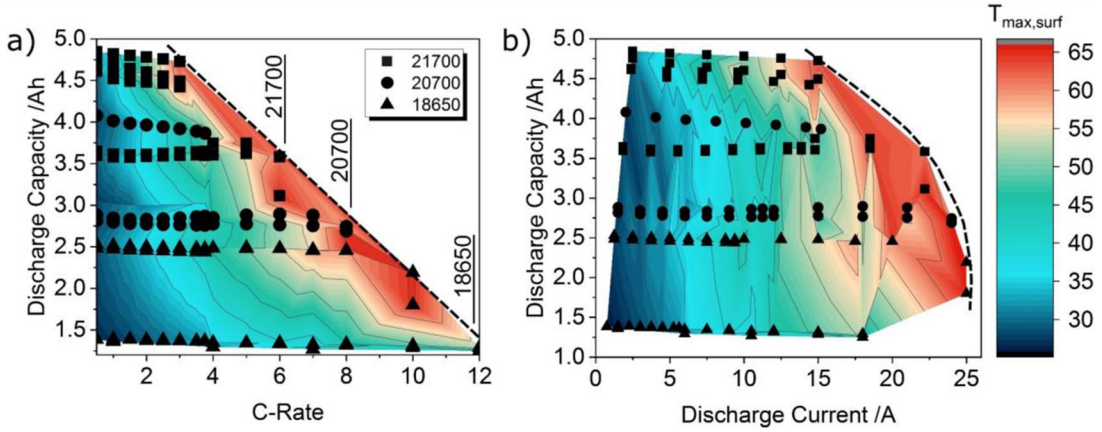

Figure 7. Discharged capacity for different 18650, 20700, and 21700 cells superimposed with temperatures at the end of discharge as a function of a) discharging C-rate and b) absolute discharge current.

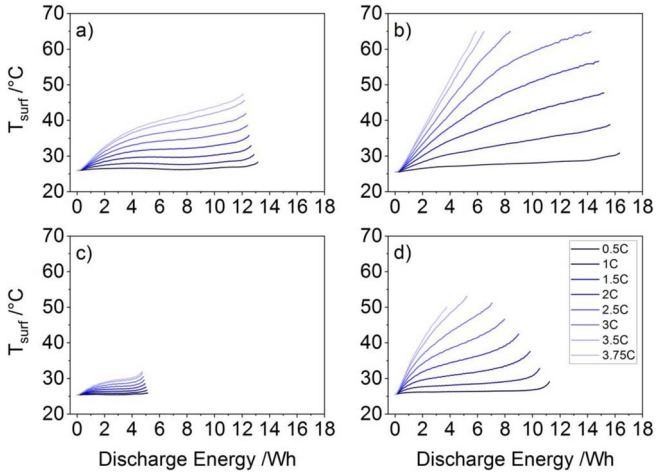

Figure 8. Temperature rise of selected 18650 and 21700 cells during current flow at an ambient temperature of 25°C. a) 21700-E1, b) 21700-H1, C) 18650-A1, d) 18650-C1.

In Figure 9a, the maximum surface temperature reached for each cell as a function of C-rate demonstrates the heating behavior of the different tested cells. The slope becomes steeper with larger cell size and higher capacity in the same format. This trend was analyzed and is shown in Figure 9b. Larger cells take longer to dissipate heat, due to the lower surface to volume ratio (∼88% for 21700 compared to 18650 cells). Cells with the same format and higher capacity have a higher ratio of active to non-active material, also making them denser and slower to dissipate heat. These physical attributes are the reason we observe a 21700 cell with 91μm anode thickness showing ∼130% of the heating rate compared to an 18650 cell at 101μm.

The ranges for the different cell formats are shown in Figure 9c for the tested cells. The regions between the high energy and high power cells of each format were shaded to represent the temperature and rate limits for each. The ranges only reflect tests performed at 25°C. Predictably, 21700 is somewhat close to 20700, and 18650 is further below.

Estimation of production effort – 21700 vs. 18650.—Analysis of industrial manufacturing processes is often difficult due to proprietary processes of competing companies. Models such as BatPac[31] attempt to calculate production costs. A cost model adopted from BatPac comparing cylindrical 18650 and 20720 cells found that cell housings contribute significantly to the total cost of production.[4] Initial SEI formation was identified as a costly step per kWh of 18650 cells due to its long time needed.[4,32]

Figure 10 shows the major production steps of cylindrical cells from materials to a pack. In a first approximation, we compare 21700 and 18650 cells regarding production effort. The basis for this rough estimation is the energy content per 21700 cell which is ∼150% compared to an 18650 cell with comparable energy density and specific energy, e.g. 18650-C (3.2 Ah, 101μm anode) and 21700-H (4.8 Ah, 91μm anode). Furthermore, very similar production equipment is taken into account, e.g. a coater, cutter, and calander that can adapt to widths of 18650 and 21700 cells. Since economy of scale was calculated to be reached above ∼1 GWh per annum,[4] a larger factory above this value was considered where scaling effects become negligible.

Cell level.—In order to produce an energy storage capability of one Wh in 18650 and 21700 cells,

1) A similar amount of electrode active materials/binder/conductive carbon black, current collectors, and separators are needed.
2) However, the number of cell housings is reduced by 33% per Wh.

Therefore, from the materials side the production cost per Wh is most likely reduced.

The following steps have to be considered in the production process:

3) Additional jellyroll windings are needed, however, less time is needed per additional winding in case the rotation speed stays the same. We note that this is likely to be a minor effect when comparing 18650 and 21700 cells. The difference would be stronger when different electrode thicknesses are compared for the same jellyroll diameter.
4) In kind with fewer cell housings, 33% fewer jellyroll insertions, electrolyte fillings, and cell closings per Wh are needed.
5) In case of a similar formation procedure, the electrical energy needed for formation per Wh will be similar. However, formation is the slowest step in the production process.[4,32] Assuming available electrical infrastructure, 33% fewer cells would undergo formation per Wh, and therefore an increase in energy output when maintaining the same number of formation stations can be expected.

Pack level.—At pack level, effort, and therefore costs, are also likely to shrink due to a lower number of cells needed to store equivalent amounts of energy:

1) 33% fewer cells are required per pack (moving cell into array, welding) in order to get the same total energy content. Pack design and module configuration should be taken into consideration, as more factors affect the number of cells needed than simply energy content at cell level. For certain applications it might even be possible to replace a pack consisting of two 18650-type cells by only one 21700 cell.
2) Fewer cells means less overhead for the BMS in case of individual cell monitoring.

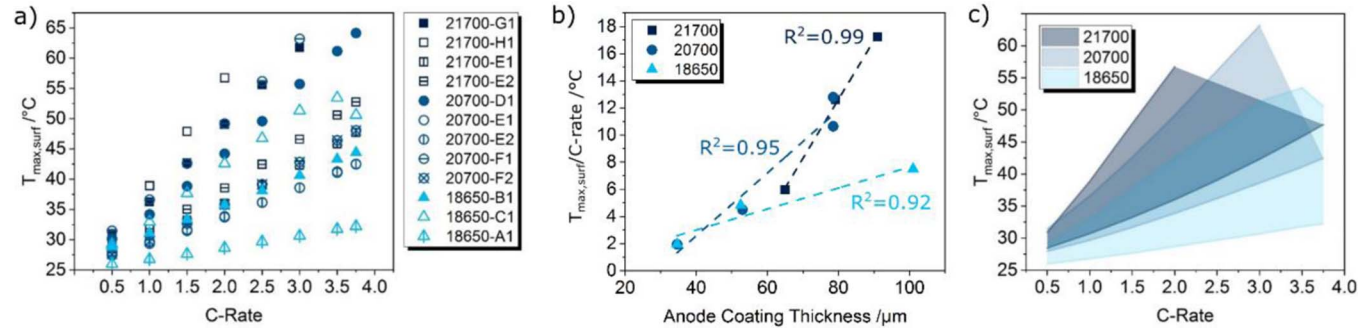

Figure 9. a) Maximum cell surface temperature reached during, or after, completion of discharge step for different commercial 18650, 20700, and 21700 cells and b) correlation of the slope in (a) with anode coating thickness. C) Observed operational temperature range for different C-rates in commercial 18650, 20700, and 21700 cells.

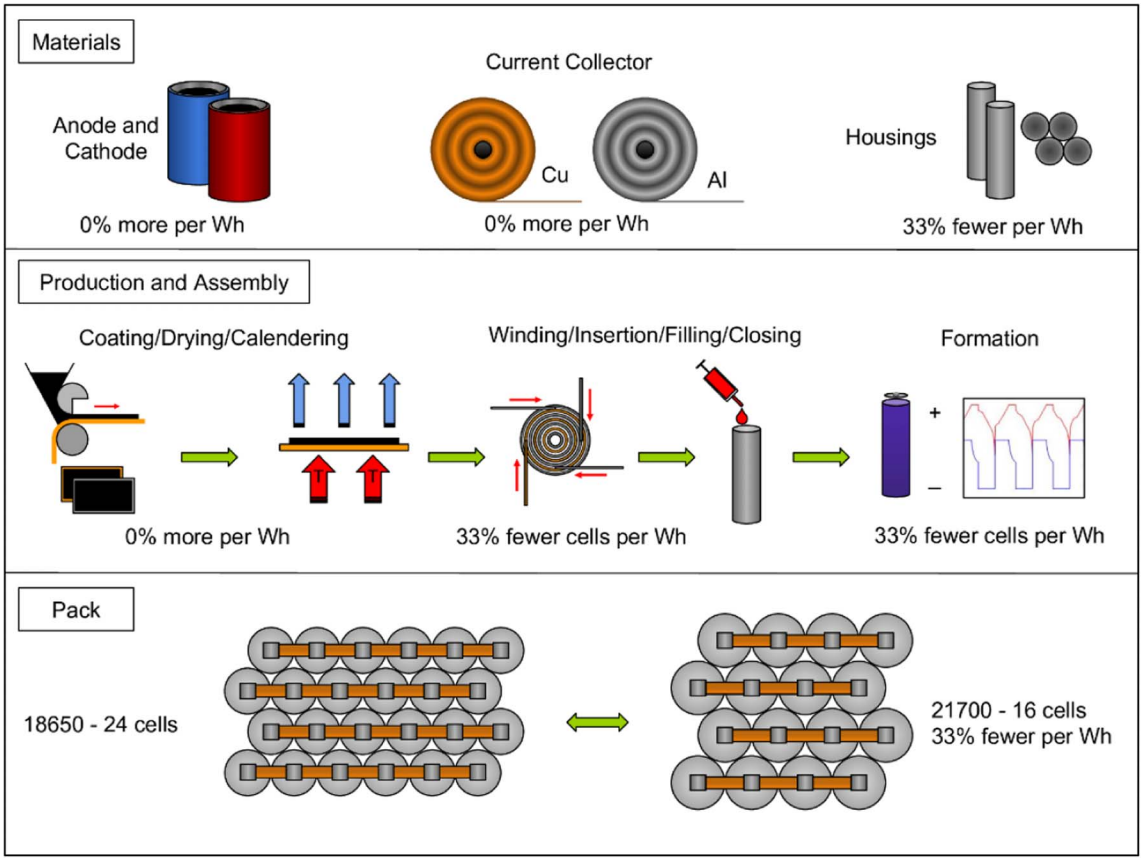

Figure 10. Material and time saving steps when changing the production from 18650 to 21700 type cells.

3) In case of a close-packed arrangement of cylindrical cells, the percentage of voids between the cells does not decrease from 18650 to 21700. Therefore, the total pack volume per Wh and the amount of cooling liquid in the voids will be similar. It is important to note a pack height increase of at least 5mm, particularly when retrofitting into existing applications.

Production line level.—On the production line level, investments are necessary to go from 18650 to 21700 cells. These investments comprise of updating the coating/cutting width, adapting/adjusting equipment for larger cell housings, including jellyroll insertion, closing, and formation stations (e.g. size and maximum current). Furthermore, it is very likely that development of electrodes fitting the new cell format will be necessary. However, adaptation of an existing line is likely to be significantly less expensive than its initial investment cost. Ideally, once production begins, up to 50% higher energy content would be produced with 21700 as for the same number of cells as 18650. We note that the numbers given above are rough estimates. Less optimistic results should be anticipated due to any number of circumstances not accounted for here.

Conclusions

We investigated several commercial types of 18650, 20700, and 21700 cells. It was found that

1) The energy content per cell can be higher by ~50% for 21700 compared to 18650. Therefore, for certain applications, less cells have to be built and used to deliver the same amount of energy.
2) The higher energy content on cell level leads to potentially lower effort and costs in the production of 21700 compared to 18650 type cells and their packs. The benefit of lower cell hardware costs is likely to be caused mainly by less cell housings, fewer jellyroll insertions/closings/tab welding, and less cell formations per Wh. More produced Wh per existing station might also have a trickledown effect on the cost.
3) The energy density does not increase significantly by changing the cell format from 18650 to 21700 type. Instead, for state-of-the-art cells, the energy density is mainly a function of the anode coating thickness, i.e. high energy cells with current material combinations usually have thicker electrodes. The study showed that it is very important to use comparable coating thicknesses or electrode loadings when comparing different active materials or at least give the coating thickness for later comparison.
4) The cell resistance is negatively influenced by the electrode thickness and positively by the electrode area. For cylindrical cells these parameters correlate with each other. This contributes to the lower performance of high energy cells. Going from the 18650 to the 21700 format, the cell resistance decreases noticeably and shows a relatively flatter correlation to anode coating thickness. The reason is the larger usable coated cathode area in the larger 21700-type cells, especially due to the outer windings of the jelly roll.
5) Increasing electrode thickness in commercial cells has a negative impact on the discharge rate capability. Cells with thicker electrodes experience higher losses by limited transport, resulting in lower discharge energy and underutilized electrode active material. The general trend for all tested cell types was found that the rate-capability is limited by the temperature on the cell surface due to current flow.

Extensive data evaluation in the present study lead to valuable new insights regarding energy density, energy content, internal resistance, and heating behavior of 21700 compared to 18650 cells. State-of-the-art 18650, 20700, and 21700 type cells are similar in their specific energy and energy density.

Our results emphasize that specific energy and energy density can mostly be enhanced on the level of materials and electrodes, i.e. new energy storage materials for future battery generations are needed. Additionally, an optimization of the electrode structure, electrolyte, formation, and cell design is necessary for each individual cell type.

A direct comparison by building 18650 and 21700 cells with the same types of electrodes is underway in our lab.

Acknowledgment

The research leading to these results has been performed within the FAB4LIB project and received funding from the German Federal Ministry of Education and Research (BMBF) under contract n° 03XP0142D. The authors thank the Project Management Agency Forschungszentrum Jülich (PTJ), Dr. R. Scurtu (ZSW) for helpful discussions, A. Fechter (ZSW) for building the pouch cells, R. Heduschka (ZSW) for conducting the CT measurement, and C. Debes (BMZ) for providing cells of type 21700-G1. J.B. Quinn and T. Waldmann contributed equally to this paper.

ORCID

Jason B. Quinn https://orcid.org/0000-0002-4478-5685
Thomas Waldmann https://orcid.org/0000-0003-3761-1668

References

1. A. Yoshino, *Angew. Chem. Int. Ed.*, **51**, 5798 (2012).
2. G. E. Blomgren, *J. Electrochem. Soc.*, **164**, A5019 (2017).
3. Panasonic, *Corp. Hist.*, accessed: 2018-05-25, https://www.panasonic.com/global/corporate/history/chronicle/1994.html.
4. R. E. Ciez and J. F. Whitacre, *J. Power Sources*, **340**, 273 (2017).
5. Samsung SDI, *SDI News*, (2017), accessed: 2018-05-25, http://www.samsungsdi.com/sdi-news/1761.html.
6. T. Waldmann, M. Wilka, M. Kasper, M. Fleischhammer, and M. Wohlfahrt-Mehrens, *J. Power Sources*, **262**, 129 (2014).
7. T. Waldmann et al., *J. Electrochem. Soc.*, **161**, A1742 (2014).
8. T. Waldmann, M. Kasper, and M. Wohlfahrt-Mehrens, *Electrochimica Acta*, **178**, 525 (2015).
9. P. J. Osswald, S. V. Erhard, J. Wilhelm, H. E. Hoster, and A. Jossen, *J. Electrochem. Soc.*, **162**, A2099 (2015).
10. P. J. Osswald et al., *J. Power Sources*, **329**, 546 (2016).
11. T. Waldmann, G. Geramifard, and M. Wohlfahrt-Mehrens, *J. Energy Storage*, **5**, 163 (2016).
12. S. S. Zhang, *J. Power Sources*, **164**, 351 (2007).
13. P. Arora, M. Doyle, and Ralph E. White, *J. Electrochem. Soc.*, **146**, 3543 (1999).
14. S. Müller et al., *J. Electrochem. Soc.*, **165**, A339 (2018).
15. S. S. Zhang, *J. Power Sources*, **162**, 1379 (2006).
16. S. Gorse et al., *Pract. Metallogr.*, **51**, 829 (2014).
17. D. P. Finegan et al., *Nat. Commun.*, **6**, 6924 (2015).
18. T. C. Bach et al., *J. Energy Storage*, **5**, 212 (2016).
19. A. Pfrang et al., *J. Power Sources*, **392**, 168 (2018).
20. X. Fleury et al., *J. Energy Storage*, **16**, 21 (2018).
21. D. A. H. McCleary, J. P. Meyers, and B. Kim, *J. Electrochem. Soc.*, **160**, A1931 (2013).
22. V. Muenzel et al., *J. Electrochem. Soc.*, **162**, A1592 (2015).
23. V. Muenzel et al., *J. Electrochem. Soc.*, **162**, Y11 (2015).
24. M. Singh, J. Kaiser, and H. Hahn, *J. Electroanal. Chem.*, **782**, 245 (2016).
25. Z. Du, D. L. Wood, C. Daniel, S. Kalnaus, and J. Li, *J. Appl. Electrochem.*, **47**, 405 (2017).
26. T. Danner et al., *J. Power Sources*, **334**, 191 (2016).
27. R. Zhao, J. Liu, and J. Gu, *Appl. Energy*, **139**, 220 (2015).
28. Y. Troxler et al., *J. Power Sources*, **247**, 1018 (2014).
29. M. Singh, J. Kaiser, and H. Hahn, *J. Electroanal. Chem.*, **782**, 245 (2016).
30. X. Zhang, *Electrochimica Acta*, **56**, 1246 (2011).
31. P. A. Nelson, K. G. Gallagher, I. Bloom, and D. W. Dees, *Gener. Energy Storage Conf.*, 116 (2017).
32. D. L. Wood, J. Li, and C. Daniel, *J. Power Sources*, **275**, 234 (2015).